Abstract

The last 8 Myr of the Cretaceous greenhouse interval were characterized by a progressive global cooling with superimposed cool/warm fluctuations. The mechanisms responsible for these climatic fluctuations remain a source of debate that can only be resolved through multi-disciplinary studies and better time constraints. For the first time, we present a record of very high-resolution (ca. 4.5 kyr) sea-surface temperature (SST) changes from the Boreal epicontinental Chalk Sea (Stevns-1 core, Denmark), tied to an astronomical time scale of the late Campanian – Maastrichtian (74 to 66 Ma). Well-preserved bulk stable isotope trends and calcareous nannofossil palaeoecological patterns from the fully cored Stevns-1 borehole show marked changes in SSTs. These variations correlate with deep-water records of climate change from the tropical South Atlantic and Pacific oceans but differ greatly from the climate variations of the North Atlantic. We demonstrate that the onset and end of the early Maastrichtian cooling and of the large negative Campanian – Maastrichtian boundary carbon isotope excursion are coincident in the Chalk Sea. The direct link between SSTs and $\delta^{13}C$ variations in the Chalk Sea reassesses long-term glacio-eustasy as the potential driver of carbon isotope and climatic variations in the Maastrichtian.

Late Cretaceous (Late Campanian – Maastrichtian) sea surface temperature record of the Boreal Chalk Sea

Nicolas Thibault[1], R. Harlou[1], N.H. Schovsbo[2], L. Stemmerik[3] and F. Surlyk[1]

[1]{Department of Geosciences and Natural Resource Management, University of Copenhagen, Øster Voldgade 10, DK-1350 Copenhagen K, Denmark}

[2]{Geological Survey of Denmark and Greenland, Øster Voldgade 10, DK-1350 Copenhagen K, Denmark}

[3]{Statens Naturhistoriske Museum, University of Copenhagen, Øster Voldgade 5–7, DK-1350 Copenhagen K, Denmark}

Correspondence to: Nicolas Thibault (nt@ign.ku.dk)

Abstract

The last 8 Myr of the Cretaceous greenhouse interval were characterized by a progressive global cooling with superimposed cool/warm fluctuations. The mechanisms responsible for these climatic fluctuations remain a source of debate that can only be resolved through multi-disciplinary studies and better time constraints. For the first time, we present a record of very high-resolution (ca. 4.5 kyr) sea-surface temperature (SST) changes from the Boreal epicontinental Chalk Sea (Stevns-1 core, Denmark), tied to an astronomical time scale of the late Campanian – Maastrichtian (74 to 66 Ma). Well-preserved bulk stable isotope trends and calcareous nannofossil palaeoecological patterns from the fully cored Stevns-1 borehole show marked changes in SSTs. These variations correlate with deep-water records of climate change from the tropical South Atlantic and Pacific

oceans but differ greatly from the climate variations of the North Atlantic. We demonstrate that the onset and end of the early Maastrichtian cooling and of the large negative Campanian – Maastrichtian boundary carbon isotope excursion are coincident in the Chalk Sea. The direct link between SSTs and $\delta^{13}C$ variations in the Chalk Sea reassesses long-term glacio-eustasy as the potential driver of carbon isotope and climatic variations in the Maastrichtian.

1 Introduction

Superimposed on the long-term cooling trend of the latest Cretaceous, two benthic foraminiferal positive oxygen isotope excursions have been documented in the early and late Maastrichtian at low and mid-latitudes of the North and South Atlantic, Indian Ocean and central Pacific (Barrera and Savin, 1999; Friedrich et al., 2009). These positive excursions, which likely reflect bottom water cooling, have been tentatively correlated to 3rd order sea-level falls and associated with changes in the mode and direction of thermohaline oceanic circulation, possibly caused by the build-up of small ephemeral Antarctic ice sheets (Barrera and Savin, 1999; Miller et al., 1999). Alternatively, these climatic changes have been associated with shifts in the source of deep water formation from low to southern high latitudes, linked to the opening of deep-sea gateways in the South Atlantic (Friedrich et al., 2009; Robinson et al., 2010; Moiroud et al., in press). In addition, the latest Maastrichtian was characterized worldwide by a brief greenhouse warming pulse, linked to Deccan volcanism (Li and Keller, 1998a; Robinson et al., 2009). This latter event is well-recorded in oxygen isotopes of benthic foraminifera but is poorly expressed in their planktonic counterparts (Li and Keller, 1998a, 1998b; Barrera and Savin, 1999; Abramovich et al., 2003). Nevertheless, changes in the marine plankton community at the end of the Maastrichtian suggest a drastic, but as

yet poorly constrained, increase in global sea-surface temperatures (SSTs, Abramovich et al., 2003; Thibault and Gardin, 2010).

Regionally divergent climatic patterns have been previously underlined in the Maastrichtian. In the southern South Atlantic, cooling was gradual, pronounced and only interrupted by the end-Maastrichtian warming (Barrera and Savin, 1999; Friedrich et al., 2009). In the North Atlantic, an apparent overall warming is inferred from low-resolution planktonic foraminiferal $\delta^{18}O$ data, while climate was globally cooling in all other oceanic basins (MacLeod et al., 2005). These regional differences emphasize the need for well-calibrated high-resolution data from different basins, and from open ocean and epicontinental seas, in order to provide a reliable picture of past climates. Data from the mid-latitude Boreal epicontinental Chalk Sea are particularly critical as this basin was connected to the north Atlantic Ocean to the west, to the Tethys to the southeast and possibly to the Arctic Ocean to the north (Fig. 1).

To investigate climate change in the Boreal Chalk Sea, we generated a calcareous nannofossil temperature index (NTI) and a new record of 1932 bulk carbonate stable isotopes across the late Campanian–Maastrichtian of the Stevns-1 core, Denmark. The sedimentology and stratigraphy of Stevns-1 have been described in detail by Rasmussen and Surlyk (2012) and Surlyk et al. (2013). Carbon isotope stratigraphic correlations with ODP Site 762C have been used to tie the Stevns-1 record to the astronomical time scale of the late Campanian–Maastrichtian (66 to 74.5 Ma, Fig. 2).

2 Methods

2.1 Age Model

The age model is based on the correlation of magnetostratigraphic records at Sites 762C and 525A and carbon isotope curves of Stevns-1, 762C and 525A as presented in Thibault et al. (2012a). Numerical ages are derived directly from the correlation with the astronomically calibrated Site 762C (Fig. 2). A small hiatus characterizes the K–Pg boundary interval in the Stevns-1 core. Another hiatus is suspected at the boundary between the Sigerslev and Højerup Members situated 2.2 m below the base Danian. Based on the comparison of global climatic trends, it is estimated here that together, these two hiatuses correspond approximately to the last 150 kyr of the Cretaceous (see section 3.3). For simplification of the age model, a total gap of 150 kyr was accounted for at the top of our record and the uppermost sample of the Maastrichtian was assigned an age of 66.15 Ma, considering an age of 66 Ma for the K-Pg boundary as in Thibault et al. (2012a). The late Campanian – Maastrichtian succession of Stevns-1 accounts for a total duration of ca. 8.15 Myr with an inferred average uncompacted sedimentation rate of 5.5 cm/kyr over the entire interval. This gives an average resolution of ca. 100 kyr for the 89 samples analyzed for nannofossil palaeoecology and ca. 4.5 kyr for the isotopic data. This oxygen isotopic dataset is the highest resolution record so far published for this interval.

2.2 Isotopic measurements and palaeotemperature reconstruction

Oxygen and carbon isotopic ratios of bulk carbonates were measured on a micromass isoprime spectrometer. Analytical precision is calculated as 0.1‰ for $\delta^{18}O$ and 0.05‰ for $\delta^{13}C$. Sea-surface temperature estimates (Fig. 3) are based on Anderson and Arthur (1983) for bulk carbonates of Stevns-1 and equation (1) of Bemis et al. (1998) for foraminiferal data of Site 525A, using a $\delta^{18}O_{sw}$ of Late Cretaceous seawater of -1.0‰ SMOW for an ice-free world. Resulting average SST estimates of ca.15.5°C in the early Maastrichtian of Denmark are in agreement with the global

compilation of Zakharov et al. (2006). In addition, we provide temperature estimates for the bulk carbonate of Stevns-1 using an average $\delta^{18}O_{sw}$ of Late Cretaceous seawater of -0.5‰ SMOW (Fig. 3) assuming glacio-eustatic variations in the range of 25–75 m in the Maastrichtian, by comparison with the extent of coincident $\delta^{18}O_{sw}$ and sea-level variations in the Oligocene to early Miocene (Billups and Schrag, 2002).

2.3 Calcareous nannofossil data

A total of 89 nannofossil slides were prepared following the method described in Thibault and Gardin (2006). Slides were analyzed for quantitative counts. Preservation of the assemblage is moderate in all samples. Relative abundances have been calculated for a total of more than 400 specimens. Our nannofossil temperature index (NTI) was calculated as the ratio between warm-water taxa and the sum of warm-water and cool-water taxa identified in the assemblage (see Section 3).

3 Results and interpretations

3.1 Calcareous nannofossils

Results from the nannofossil analysis are focused here primarily on potential temperature changes as expressed in the nannofossil assemblage through the abundance of cool- and warm-water taxa. *Ahmuellerella octoradiata*, *Gartnerago* spp., *Kamptnerius magnificus*, and *Nephrolithus frequens* are considered as high-latitude taxa, and *Arkhangelskiella cymbiformis* sensu lato has a greater affinity to cool-waters (Wind, 1979; Thierstein, 1981; Pospichal and Wise, 1990; Watkins, 1992; Lees, 2002; Thibault and Gardin, 2006, 2010). *Watznaueria barnesiae* is ubiquitous in Cretaceous

assemblages. Several studies have demonstrated that this is a low-nutrient indicator (Erba et al., 1992; Williams and Bralower, 1995). However, during the Maastrichtian, varying abundances and patterns of migration of this species in mid- and high-latitudes have mainly been linked to temperature changes (Watkins, 1992; Sheldon et al., 2010). Sheldon et al. (2010) and Thibault et al. (2015) have shown that warm intervals in the Boreal Chalk Sea are characterized by an increase in abundance of *W. barnesiae*. Cool-water taxa and *W. barnesiae* clearly show opposite long-term trends throughout the studied succession and highlight three warm intervals in the late Campanian, mid-Maastrichtian and latest Maastrichtian, and two cool intervals in the early and late Maastrichtian (Fig. 3). The palaeoecological affinity of *Ahmuellerella regularis* is unknown and this species is has shown to be common both in the tropical and mid-latitude areas. However, in the Stevns-1 core, intervals with lower abundances of high-latitude taxa and higher abundances in *W. barnesiae* also show enrichments in *A. regularis* (Fig. 3). Therefore, in this study, this species was grouped together with *W. barnesiae* among the warm-water taxa. Our Nannofossil Temperature Index (NTI) was calculated as follows:

NTI = (% *W. barnesiae* + % *A. regularis*) / [(% *A. cymbiformis* s.l. + % *A. octoradiata* + % *Gartnerago* spp. + % *K. magnificus* + % *N. frequens*)+(% *W. barnesiae*+% *A. regularis*)].

(1)

Note that the applicability of the NTI developed here is restricted to the Campanian–Maastrichtian interval and should preferably remain valid for the Boreal realm only as the composition of the calcareous nannofossil assemblage is significantly different in the Tropical realm.

3.2 Validation of Stevns-1 bulk $\delta^{18}O$ as a proxy for Late Cretaceous SSTs

The nannofossil chalk of the Danish Basin is a very pure carbonate. Carbonate content of the analyzed bulk rock samples is generally over 95% in all analyzed samples. Scanning electron microscope images of the chalk show numerous calcareous nannofossils with dissolution phenomenon, little recrystallization and small carbonate micro-particles, which likely come from the breakdown of nannofossils (Fig. 4). Despite its controversial use, a number of studies have demonstrated the usefulness of bulk pelagic/hemipelagic carbonate oxygen stable isotope data for SST reconstruction (Jarvis et al., 2011; Jarvis et al., in press; Reghellin et al., 2015). Recent experiments have shown reduced coccolithophore interspecific differences and less carbon and oxygen-isotope fractionation in large and slow growing species with higher ambient carbon availability, which is expected in the sea water of periods with high CO_2 concentrations such as the Cretaceous (Rickaby et al., 2010; Bolton et al., 2012; Hermoso et al., 2014). It has been recently proven that coccolithophore vital effects actually vanish at high pCO_2 regimes, thus supporting the use of non-altered bulk nannofossil chalk as an excellent calcitic material for $\delta^{18}O$ analysis as a proxy for SSTs, despite recent years of neglect and favor to species-specific planktic foraminifer $\delta^{18}O$ (Hermoso et al., 2016). Due to its limited diagenetic alteration, the nannofossil chalk of Stevns-1 may thus draw a reliable picture of sea-surface water environmental conditions.

The NTI and $\delta^{18}O$ values of Stevns-1 show similar trends for the late Campanian–Maastrichtian (Fig. 3). In order to test the correlation between low-resolution nannofossil and high-resolution isotopic data, both 7 and 21 point running averages were run over $\delta^{18}O$ values. Correlation was tested for the resulting values of the 89 samples in common. The R^2 Pearson coefficient of correlation between the NTI and the $\delta^{18}O$ is 0.60 for the 7 point running average and increases up to 0.69 for a 21 point running average. This suggests temperature (and possibly continental ice growth driven changes in seawater $\delta^{18}O$) as the dominant(s) factor(s) controlling the observed variations in the bulk $\delta^{18}O$ of Stevns-1. Little influence of diagenesis is reinforced by the lack of correlation

between $\delta^{18}O$ and $\delta^{13}C$ data of this core (Thibault et al., 2012b). The timing and magnitude of long-term $\delta^{18}O$ changes at Stevns-1 match those recorded in benthic foraminiferal data at Site 525A (Li and Keller, 1998a, 1998b) as well as $\delta^{18}O$ variations observed in planktonic foraminifer *Globotruncana arca* from the late Campanian to the mid-Maastrichtian (Friedrich et al., 2009) (Fig. 5). The preservation of $\delta^{18}O$ trends, the good correlation with the NTI and the consistent palaeotemperature estimates argue against the influence of prominent diagenetic alteration in the chalk of Stevns-1. The $\delta^{18}O$ record of Stevns-1 can thus be used as a proxy to describe Late Cretaceous SSTs in the Chalk Sea.

3.3 Climatic trends

Calcareous nannofossil and $\delta^{18}O$ data from Stevns-1 suggest the following climatic evolution in the Chalk Sea: From 73.8 and 72.8 Ma, a late Campanian climatic warm optimum with SSTs between ca. 19 and 20°C, followed by a late Campanian – early Maastrichtian progressive cooling of 3.5°C (Fig. 5). From 72.8 to 71 Ma, cooling occurs in two major phases, interrupted by a ca. 600 kyr long stable period. These two long cooling steps are characterized by rapid temperature drops, two of which can also be observed in the NTI at 72.8 and at 72–71.8 Ma. A cool climate mode with slight oscillations in SSTs around 15.5°C is recorded between 71 and 69.8 Ma. The transition between the early Maastrichtian cooling and mid-Maastrichtian warming is characterized by a rapid 1.5°C increase in SSTs lasting ca. 300 kyr at 69.8–69.5 Ma. The mid-Maastrichtian warming trend is characterized by SSTs oscillating around 16.5 to 17°C between 69.5 and 68.4 Ma. This trend is followed by a late Maastrichtian cooling of 1°C during which minimal SSTs around 15.5°C at 67.9 Ma are reached. A concomitant sharp decrease in $\delta^{18}O$ and increase of the NTI delineate the end-Maastrichtian warming from ca. 66.3 Ma up to the K–Pg boundary. This last warming episode

accounts for a total of 2°C in the Boreal Realm and occurs in two rapid (<100 kyr) steps of 1°C each at ca. 66.3 and 66.2 Ma (Fig. 5).

The K–Pg boundary clay is not present in the Stevns-1 core, which suggests a small gap across the K–Pg boundary interval. This small gap is only local, as small basins are developed across the K–Pg boundary. Sections through these basins show a complete development of the K–Pg succession, whereas sections between the basins contain a small gap spanning the boundary transition and in the order of several tens of centimetres, i.e. <30 kyr (Surlyk et al., 2006). In addition, the presence of a double incipient hardground at the base of the Højerup Member, situated 4 to 5 metres below the K–Pg boundary at Stevns Klint, suggests another potential hiatus within the uppermost Maastrichtian interval (Surlyk et al., 2006). These small gaps in Stevns-1 partly hinder observation of a globally characterized short cooling event immediately before the K–Pg event (Li and Keller, 1998a; Thibault and Gardin, 2010; Punekar et al., 2014; Thibault and Husson, 2015). The duration of this end-Cretaceous cooling episode has been estimated to be of the order of 100 to 120 kyr and is followed by a ca. 30 kyr short pulse of warming in the Tethys (Punekar et al., 2014; Thibault and Husson, 2015).

A sharp decrease in the relative abundance of *W. barnesiae* and in the NTI situated within the Højerup Mb. suggests that the onset of the last end-Cretaceous cooling episode is present in the core (Fig. 3). Therefore, the cumulated uppermost Maastrichtian gap in the Stevns-1 core is of a limited extent, corresponding to less than 150 kyr of the latest Cretaceous and most of it probably corresponds to the double incipient hardground.

4 Discussion

Despite regional differences between the South Atlantic and the Chalk Sea, climatic trends generally match well (Fig. 5). Except for the North Atlantic, low and mid-latitudes of all other oceanic basins show the same climate modes (Barrera and Savin, 1999; MacLeod et al., 2005) that appear to be related to coeval changes in atmospheric pCO_2 (Nordt et al., 2003; Gao et al., 2015). Differences in climate trends between the Chalk Sea and the North Atlantic are difficult to reconcile with their tight connection and multiple gateways across submerged parts of UK and the Paris Basin (Fig. 1). However, Maastrichtian water masses at the location of Stevns-1 could have been influenced by Tethyan northwestward currents, as suggested by the direction of large channels in seismic profiles offshore Stevns Klint and further north in the Danish Basin (Lykke-Andersen and Surlyk, 2004; Esmerode et al., 2007; Surlyk and Lykke-Andersen, 2007).

Climatic trends from Stevns-1 correlate with $\delta^{18}O$ trends of benthic foraminifers at Site 525A (Walvis Ridge, South Atlantic), which represents the highest resolution record on separated foraminifers for this time interval (Li and Keller, 1998a, 1998b; Friedrich et al., 2009) (Fig. 5). SSTs in the Chalk Sea followed the same evolution as intermediate and deep-waters of the South Atlantic, Indian Ocean and central Pacific (Barrera and Savin, 1999). However, the record of most planktonic foraminifers in these basins fails to clearly depict the trends in sea-surface waters (Barrera and Savin, 1999; Li and Keller, 1999). Stevns-1 bulk $\delta^{18}O$ and calcareous nannofossil assemblages, as well as $\delta^{18}O$ values of *G. arca* at Site 525A indicate that climatic modes recorded in late Campanian – Maastrichtian intermediate and deep waters affected sea surface waters in a similar fashion (Fig. 5). Changes in Maastrichtian nannofossil assemblages in the tropical Atlantic and Pacific oceans delineate the same climatic trends in sea-surface waters (Thibault and Gardin, 2006, 2010). Migration patterns in planktonic organisms throughout the late Campanian–Maastrichtian strengthen this interpretation (Watkins, 1992; Thibault et al., 2010).

When comparing $\delta^{18}O$ values of planktonic foraminifers *Rugoglobigerina rugosa* and *Globotruncana arca* at Site 525A across the early Maastrichtian cooling, it appears that data from the latter species show a better consistency with variations observed in the benthic foraminiferal record and in the bulk of Stevns-1 (Fig. 5). This suggests that $\delta^{18}O$ values of *R. rugosa* likely reflect underestimated and smoothed SST variations in the late Campanian – Maastrichtian interval, whereas data acquired on *G. arca* reflect a more faithful picture of primary Late Cretaceous South Atlantic SSTs. Potential diagenetic overprint, the presence of numerous pseudo-cryptic ecophenotypes of *Rugoglobigerina* and vital effect associated to photosymbiosis can be invoked to explain this discrepancy in the $\delta^{18}O$ values of *R. rugosa* (Abramovich et al., 2003; Falzoni et al., 2014).

Despite these similarities, regional differences are nevertheless apparent across the early Maastrichtian cooling event between Stevns-1 (palaeolatitude: 45°N) and Site 525A (palaeolatitude: 36°S). A short warming pulse occurs in the middle of this interval at Site 525A (Fig. 5). This pulse is very poorly recorded at Stevns-1 through a number of outlying data points with lighter values between -252 and -272 m (Fig. 3) and through slightly lighter values in the 2 standard deviation envelope of Stevns-1 between 70.45 and 70.85 Ma (Fig. 5). The nannofossil assemblage of Stevns-1 does not appear to show any warming in this interval. However, a similar short pulse of warming has been recorded during the early Maastrichtian cooling through lighter values of the bulk $\delta^{18}O$ accompanied by a slight enrichment in *Watznaueria barnesiae* in the Skælskør-1 core (SW Sjælland, Denmark, Thibault et al., 2015).

Comparison of the Stevns-1 $\delta^{13}C$ and $\delta^{18}O$ data sheds new light on the relationship between the large negative carbon isotope excursion (CIE) of the Campanian–Maastrichtian boundary interval and the early Maastrichtian cooling. The onset of progressive cooling at 72.8 Ma coincides exactly with the onset of the decrease in $\delta^{13}C$ values, while the onset of the early Maastrichtian warming

mode is broadly coeval to the top of the recovery in $\delta^{13}C$ values at 69.5 Ma (Fig. 3). It was recently shown that the negative $\delta^{13}C$ excursion predates the $\delta^{18}O$ increase with a lag of about 600 kyr at Sites 525A and 690 (Weddell Sea, Southern Ocean) (Friedrich et al., 2009). In contrast, our new high-resolution dataset actually supports synchroneity between the CIE and the positive $\delta^{18}O$ excursion of this interval. Isotopic data from Site 525A neither confirm or refute this observation because data from the onset of the excursion at 73 Ma are lacking. However, the return to a mid-Maastrichtian warm mode at 69.5 Ma is coincident with a rapid increase in the $\delta^{13}C$ of benthic and planktonic foraminifers at Site 525A (Fig. 2). Therefore, it is possible that the lag between the two signals is a Southern Ocean phenomenon. Decoupling between the two signals can, however, be highlighted at Stevns-1 elsewhere in the record. For example, the stepwise decrease in $\delta^{13}C$ between 73 and 71 Ma appears to be decoupled from the $\delta^{18}O$ record (Fig. 3). Here, maximum cooling occurs between 71.5 and 69.5 Ma during a progressive rise in $\delta^{13}C$ values. This decoupling remains to be explained, but with respect to the onset and termination of $\delta^{18}O$ and $\delta^{13}C$ excursions, our results argue for a direct cause and effect scenario in the Chalk Sea.

Decoupling and lead-lag relationships between these two proxies has been used as an argument to rule out Maastrichtian glaciation and a subsequent drop in sea level as a likely scenario for these two isotopic excursions (Friedrich et al., 2009). On the contrary, our results tend to show consistency with a glacio-eustatic scenario as previously supported by Barrera and Savin (1999) and Miller et al. (1999). Despite the fact that Kominz et al. (2008) used the Geologic Time Scale 2004 with the K–Pg and Campanian–Maastrichtian boundaries at respectively 65.5 and 70.6 Ma, respectively, comparison of the timing of the two cooling episodes appears to match fairly well with that of the two major lowstands in the New Jersey margin sea-level curve (Kominz et al., 2008; Fig. 5). Haq (2014) recently identified six 3rd order sea-level cycles in the late Campanian – Maastrichtian interval bounded by sequence boundaries (SBs) KCa7, KMa1, KMa2, KMa3, KMa4

and KMa5, among which KMa2 and KMa5 at 70.6 and 66.8 Ma, respectively, are considered as major cycle boundaries. Considering the great uncertainty in the estimated ages of Haq's SBs, the timing of major SBs KMa2 and KMa5 at 70.6 and 66.8 Ma corresponds well to a position within the two lowstands of the New Jersey record and within the cooling episodes highlighted at Stevns-1 (Fig. 5). A number of third-order sea-level regressions of the mid-Cretaceous greenhouse have been recently explained through aquifer-eustasy (Wagreich et al., 2014; Wendler and Wendler, 2016; Wendler et al., 2016). However, such regressions correlate to climatic warming episodes and this new model for sea-level change can thus not explain the relationship between global cooling and 3rd order sea-level fall mentioned here for the Maastrichtian (Wendler and Wendler, 2016; Wendler et al., 2016).

Although no direct evidence of glaciation, such as dropstones and ice-rafted debris, have been found in the late Campanian–Maastrichtian of the Southern Ocean (Price et al., 1999), examination of diatom-rich sediments from the Alpha Ridge, and palynomorph records from southeastern Australia and Seymour Island support the development of winter sea ice in the Arctic Sea and around Antarctica, and the waxing and waning of ephemeral Antarctic ice sheets at that time (Gallagher et al., 2008; Davies et al., 2009; Bowman et al., 2013). The development of ephemeral ice sheets in Antarctica can explain the $\delta^{18}O$ excursions through a drop in seawater $\delta^{18}O$ accompanied by a global cooling of water masses (Barrera and Savin, 1999; Li and Keller, 1999). Sea-level changes could trigger the onset and termination of the late Campanian – early Maastrichtian CIE by shifting calcium carbonate accumulation and organic-matter burial from shelf to open-ocean areas (Barrera and Savin, 1999; Friedrich et al., 2009). The occurrence of the CIE and the early Maastrichtian cooling have been recently explained mainly by a global change in the source of intermediate and deep-water masses and the onset of deep-water formation in the Southern Ocean, favoured by the opening of tectonic gateways (Robinson et al., 2010; Koch and

Friedrich, 2012). However, a reorganization in the global oceanic circulation is actually compatible with a glacio-eustatic scenario and could have been triggered both by tectonics and glaciation. In such a scenario, changes in the sea-water $\delta^{18}O_{sw}$ within a range of 25 to 75 m glacio-eustatic variations may have followed a rather similar evolution as for the Oligocene–Miocene interval (Billups and Schrag, 2002). Palaeotemperature calculations should progressively and cyclically shift from an equation that assumes a sea-water $\delta^{18}O$ ($\delta^{18}O_{sw}$) of -1‰ to potential $\delta^{18}O_{sw}$ down to ca.-0.5‰ (Billups and Schrag, 2002). Minimum temperatures of 15.5°C for the SSTs of the Boreal Chalk Sea during the early and late Maastrichtian coolings could thus be underestimated and may rather be around 17.5°C (Figs. 3 and 5).

5 Conclusions

High-resolution bulk stable isotopes and calcareous nannofossil data from the fully cored Stevns-1 borehole provide fundamental insights into the late Campanian – Maastrichtian climate of the Boreal Chalk Sea. Our results show that the evolution of SSTs in the Boreal Chalk Sea parallel that of bottom-water temperatures at low and mid-latitudes of the North and South Atlantic, Indian Ocean and central Pacific. Two major cool intervals are highlighted at 71.6–69.6 (lower Maastrichtian) and 67.9–66.4 Ma (upper Maastrichtian). The onset and end of the late Campanian – early Maastrichtian negative CIE are coincident with the onset of cooling in the late Campanian and with the onset of the mid-Maastrichtian warming, respectively. These data reopen the possibility of a Maastrichtian glacio-eustatic scenario, supporting a causal relationship between changes in eustatic sea level and major shifts in Late Cretaceous $\delta^{13}C$ as previously suggested by Jarvis et al. (2002). Assuming that the early and late Maastrichtian coolings were caused by glaciation, palaeotemperature estimates should be calculated with two different equations using either a $\delta^{18}O_{sw}$

of -1‰ during warm episodes or a $\delta^{18}O_{sw}$ of ca.-0.5‰ during cool episodes. In such a scenario, the full extent of the early Maastrichtian SST cooling would thus be 4°C rather than 6°C. Finally, the two sharp stepwise 1°C increases in SSTs of the Chalk Sea at 66.3 and 66.2 Ma are consistent with the second main phase of the Deccan volcanic episode in a series of rapid pulses of flood basalt volcanism and associated release of greenhouse gases (Chenet et al., 2009).

Acknowledgments

Funding for this study was provided by the Danish Natural Science Research Council, the Natural Science Faculty, the University of Copenhagen and the Carlsberg Foundation. We thank C.V. Ullmann, J. Moreau, M. Ruhl, and D. Husson for fruitful discussions as well as Michael Wagreich and Ian Jarvis for their useful comments and suggestions on the article.

References

Abramovich, S., Keller, G., Stüben, D., and Berner, Z.: Characterization of late Campanian foraminiferal depth habitats and vital activities based on stable isotopes, Palaeogeogr. Palaeoclimatol. Palaeoecol., 202, 1–29, 2003.

Anderson, T.F. and Arthur, M.A.: Stable isotopes of oxygen and carbon and their application to sedimentologic and environmental problems, in: Stable isotopes in sedimentary geology, edited by: Arthur, M.A. et al., SEPM Short Course Notes, 10, 1–151, 1983.

Barrera, E. and Savin, S.M.: Evolution of late Campanian–Maastrichtian marine climates and oceans, in: Evolution of the Cretaceous ocean-climate system, edited by: Barrera E. and Johnson C.C., GSA Special Paper, 332, 245–282, doi:10.1130/0-8137-2332-9.245, 1999.

Bemis, B.E., Spero, H.J., Bijma, J. and Lea, D.W.: Reevaluation of the oxygen isotopic composition of planktonic foraminifera: Experimental results and revised paleotemperature equations. Paleoceanography. 13, 150–160, doi:10.1029/98PA00070, 1998.

Billups, K. and Schrag, D.P.: Paleotemperatures and ice volume of the past 27 Myr revisited with paired Mg/Ca and 18O/16O measurements on benthic foraminifera. Paleoceanography, 17, doi: 10.1029/2000PA000567, 2002.

Bolton, C.T., Stoll, H.M. and Mendez-Vicente, A.: Vital effects in coccolith calcite: Cenozoic climate-pCO2 drove the diversity of carbon acquisition strategies in coccolithophores? Paleoceanography, 27. doi: 10.1029/2012PA002339, 2012.

Bowman, V.C., Francis, J.E. and Riding, J.B.: Late Cretaceous winter sea ice in Antarctica ? Geology, 41, 1227–1230, 2013.

Chenet, A.-L., Courtillot, V., Fluteau, F., Gérard, M., Quidelleur, X., Khadri, S.F.R., Subbarao, K.V. and Thordarson, T.: Determination of rapid Deccan eruptions across the Cretaceous- Tertiary boundary using paleomagnetic secular variation: 2. Constraints from analysis of eight new sections and synthesis for a 3500-m-thick composite section, J. Geophys. Res., 114, B6103, doi:10.1029/2008JB005644, 2009.

Davies, A., Kemp, A.E.S. and Pike, J.: Late Cretaceous seasonal ocean variability from the Arctic, Nature, 460, 254–258, 2009.

Erba, E., Castradori, F., Guasti, G. and Ripepe, M.: Calcareous nannofossils and Milankovitch cycles: the example of the Gault Clay Formation (southern England), Palaeogeogr. Palaeoclimatol. Palaeoecol., 93, 47–69, 1992.

Esmerode, E.V., Lykke-Andersen, H. and Surlyk, F.: Ridge and valley systems in the Upper Cretaceous chalk of the Danish Basin: contourites in an epireic sea, in: Economic and Palaeoceanographic Significance of Contourite Deposits, edited by: Viana, A.R. and Rebesco, M., Geological Society of London Special Publication, 276, 265–282, 2007.

Falzoni, F., Petrizzo, M.R., Huber, B.T. and MacLeod, K.G.: Insight into the meridional ornamentation of the planktonic foraminiferal genus Rugoglobigerina (Late Cretaceous) and implications for taxonomy, Cretaceous Res., 47, 87–104, 2014.

Friedrich O., Herrle J.O., Cooper M.J., Erbacher J., Wilson P.A. and Hemleben C.: The early Maastrichtian carbon cycle perturbation and cooling event: Implications from the South Atlantic Ocean, Paleoceanography, 24, PA221, doi:1012/2008PA001654, 2009.

Gallagher, S.J., Wagstaff, B.E:, Barid, J.G., Wallace, M.W. and Li, C.L.: Southern high latitude climate variability in the Late Cretaceous greenhouse world, Global Planet. Change, 60, 351–364, 2008.

Gao, Y., Ibarra, D.E., Wang, C., Caves, J.K., Chamberlain, C.P., Graham, S.A. and Wu, H.: Mid-latitude terrestrial climate of East Asia linked to global climate in the Late Cretaceous. Geology, 43, 287–290, 2015.

Haq, B., U., Cretaceous Eustasy revisited, Global Planet. Change, 113, 44–58, 2014.

Hermoso, M., Horner, T.J., Minoletti, F. and Rickaby, R.E.M.: Constraints on the vital effect in coccolithophore and dinoflagellate calcite by oxygen isotopic modification of seawater. Geochim. Cosmochim. Ac., 141, 612–627, 2014.

1 Hermoso, M., Chau, I.Z.X., McClelland, H.L.O., Heureux, A.M.C. and Rickaby, R.E.M.:
2 Vanishing coccolith vital effect with alleviated carbon limitation. Biogeosciences, 13, 1–12,
3 doi:10.5194/bg-13-1-2016, 2016.

4 Jarvis, I., Mabrouk, A., Moody, R.T.J. and de Cabrera, S.: Late Cretaceous (Campanian) carbon
5 isotope events, sea-level change and correlation of the Tethyan and Boreal realms, Palaeogeogr.
6 Palaeoclimatol. Palaeoecol., 188, 215–248, 2002.

7 Jarvis, I., Lignum, J.S., Gröcke, D.R., Jenkyns, H.C. and Pearce, M.A.: Black shale deposition,
8 atmospheric CO2 drawdown, and cooling during the Cenomanian-Turonian Oceanic Anoxic Event.
9 Paleoceanography, 26, doi: 10.1029/2010PA002081, 2011.

10 Jarvis, I., Trabucho-Alexandre, J., Gröcke, D.R., Ulicny, D. and Laurin, J.: Intercontinental
11 correlation of organic carbon and carbonate stable isotope records: evidence of climate and sea-
12 level change during the Turonian (Cretaceous), The Depositional Record, doi: 10.1002/dep2.6, in
13 press.

14 Koch, M. C. and Friedrich, O.: Campanian–Maastrichtian intermediate- to deep-water changes in
15 the high latitudes: Benthic foraminiferal evidence, Paleoceanography, 27, PA2209,
16 doi:10.1029/2011PA002259, 2012.

17 Kominz, M.A., Browning, J.V., Miller, K.G., Sugarman, P.J., Mizintsevaw, S. and Scotese, C.R.:
18 Late Cretaceous to Miocene sea-level estimates from the New Jersey and Delaware coastal plain
19 coreholes: an error analysis, Basin Res., 20, 211–226, 2008.

20 Laskar, J., Fienga, A., Gastineau, M. and Manche, H.: La2010: A new orbital solution for the long-
21 term motion of the Earth, Astron. Astrophys. 532, A89, doi:10.1051/0004-6361/201116836, 2011.

1 Lees, J.A.: Calcareous nannofossils biogeography illustrates palaeoclimate change in the Late
2 Cretaceous Indian Ocean, Cretaceous Res., 23, 537–634, 2002.

3 Li, L. and Keller, G.: Abrupt deep-sea warming at the end of the Cretaceous, Geology, 26, 995–998,
4 1998a.

5 Li, L. and Keller, G.: Maastrichtian climate, productivity and faunal turnovers in planktic
6 foraminifera in South Atlantic DSDP sites 525A and 21, Mar. Micropaleontol., 33, 55–86, 1998b.

7 Li, L. and Keller, G.: Variability in Late Cretaceous and deep waters: evidence from stable isotopes,
8 Mar. Geol., 161, 171–190, 1999.

9 Lykke-Andersen, H. and Surlyk, F.: The Cretaceous–Paleogene boundary at Stevns Klint,
10 Denmark: inversion tectonics or sea-floor topography ?, J. Geol. Soc. London, 161, 343–352, 2004.

11 MacLeod, K. G., Huber, B.T. and Isaza-Londoño, C.: North Atlantic warming during global cooling
12 at the end of the Cretaceous, Geology, 33, 437–440, 2005.

13 Markwick, P.J. and Valdes, P.J.: Palaeo-digital elevation models for use as boundary conditions in
14 coupled ocean–atmosphere GCM experiments: a Maastrichtian (late Cretaceous) example.
15 Palaeogeogr. Palaeoclimatol. Palaeoecol., 213, 3763, 2004.

16 Miller, K.G., Barrera, E., Olsson, R.K., Sugarman, P.J. and Savin, S.M.: Does ice drive early
17 Maastrichtian eustasy?, Geology, 27, 783–786, 1999.

18 Moiroud, M., Pucéat, E., Donnadieu, Y., Bayon, G., Guiraud, M., Voigt, S., Deconinck, J.-F. and
19 Monna, F.: Evolution of neodymium isotopic signature of seawater during the Late Cretaceous:
20 Implications for intermediate and deep circulation. Gondwana Research, doi:
21 10.1016/j.gr.2015.08.005, in press.

1 Pospichal, J.J. and Wise Jr., S.W.: Calcareous nannofossils across the K–T boundary, ODP Hole
2 690C, Maud Rise, Weddell Sea, Proc. Ocean Drill. Program. Sci. Results, 113, 515–532, 1990.

3 Price, G.D.: The evidence and implications of polar ice during the Mesozoic, Earth-Sci. Rev., 48,
4 183–210, 1999.

5 Punekar, J., Mateo, P. and Keller, G.: Effects of Deccan volcanism on paleoenvironment and
6 planktic foraminifera: a global survey, in: Volcanism, impacts, and mass extinctions: causes and
7 effects, edited by: Keller, G. and Kerr, A.C., GSA Spec. Pap., 505, 91–116, 2014.

8 Rasmussen, S.L. and Surlyk, F.: Facies and ichnology of an Upper Cretaceous chalk contourite drift
9 complex, eastern Denmark, and the validity of contourite facies models, J. Geol. Soc. London, 169,
10 435-447, 2012.

11 Reghellin, D., Coxall, H.K., Dickens, G.R. and Backman, J.: Carbon and Oxygen isotopes of bulk
12 carbonate in sediment deposited beneath the eastern equatorial Pacific over the last 8 million years,
13 Paleoceanography, 30, 1261–1286, doi:10.1002/2015PA002825, 2015.

14 Rickaby, R.E.M., Henderiks, J. and Young, J.N.: Perturbing phytoplankton: response and isotopic
15 fractionation with changing carbonate chemistry in two coccolithophore species, Clim. Past, 6, 771–
16 785, 2010.

17 Robinson, N., Ravizza, G., Coccioni, R., Peucker-Ehrenbrink, B. and Norris, R.: A high resolution
18 marine 187Os/188Os record for the late Maastrichtian: distinguishing the chemical fingerprints of
19 Deccan volcanism and the KP impact event, Earth Planet. Sci. Lett., 281, 159–168, 2009.

20 Robinson, S.A., Murphy, D.P., Vance, D. and Thomas, D.J.: Formation of "Southern Component
21 Water" in the Late Cretaceous: evidence from Nd-isotopes, Geology, 38, 871–874, 2010.

Sheldon, E., Ineson, J. and Bown, P.: Late Maastrichtian warming in the Boreal Realm: Calcareous nannofossil evidence from Denmark, Palaeogeogr. Palaeoclimatol. Palaeoecol., 295, 55–75, 2010.

Surlyk, F., Dons, T., Clausen, C.K. and Higham, J.: Upper Cretaceous, in: The Millennium Atlas: petroleum geology of the central and northern North Sea, edited by: Evans, D., Graham, C., Armour, A. and Bathurst, P., The Geological Society, London, 213–233, 2003.

Surlyk, F., Damholt, T. and Bjerager, M., Stevns Klint, Denmark: Uppermost Maastrichtian chalk, Cretaceous–Tertiary boundary, and lower Danian bryozoan mound complex. B. Geol. Soc. Denmark, 54, 1–48, 2006.

Surlyk, F., Rasmussen, S.L., Boussaha, M., Schiøler, P., Schovsbo, N.H., Sheldon, E., Stemmerik, L and Thibault, N.: Upper Campanian–Maastrichtian holostratigraphy of the eastern Danish Basin, Cretaceous Res., 46, 232–256, 2013.

Thibault, N. and Gardin, S.: Maastrichtian calcareous nannofossil biostratigraphy and paleoecology in the Equatorial Atlantic (Demerara Rise, ODP Leg 207 Hole 1258A), Rev. Micropaleontol., 49, 199–214, 2006.

Thibault, N. and Gardin, S.: The calcareous nannofossil response to the end-Cretaceous warm event in the Tropical Pacific, Palaeogeogr. Palaeoclimatol. Palaeoecol., 291, 239–252, 2010.

Thibault, N., Gardin, S. and Galbrun, B.: Latitudinal migration of calcareous nannofossil Micula murus in the Maastrichtian: Implications for global climate change, Geology, 38, 203–206, 2010.

Thibault, N., Husson, D., Harlou, R., Gardin, S., Galbrun, B., Huret, E. and Minoletti, F.: Astronomical calibration of upper Campanian–Maastrichtian carbon isotope events and calcareous plankton biostratigraphy in the Indian Ocean (ODP Hole 762C): Implication for the age of the

Campanian–Maastrichtian boundary, Palaeogeogr. Palaeoclimatol. Palaeoecol., 337–338, 52–71, 2012a.

Thibault, N., Harlou, R., Schovsbo, N., Schiøler, P., Minoletti, F., Galbrun, B., Lauridsen, B.W., Sheldon, E., Stemmerik, L. and Surlyk, F.: Upper Campanian–Maastrichtian nannofossil biostratigraphy and high-resolution carbon-isotope stratigraphy of the Danish Basin: towards a standard δ13C curve for the Boreal Realm, Cretaceous Res., 33, 72–90, 2012b.

Thibault, N., Anderskouv, K., Bjerager, M., Boldreel, L.O., Jelby, M.E., Stemmerik, L. and Surlyk, F.: Upper Campanian–Maastrichtian chronostratigraphy of the Skælskør-1 core, Denmark: correlation at the basinal and global scale and implications for changes in sea-surface temperatures, Lethaia, 48, 549–560, doi: 10.1111/let.12128, 2015.

Thibault, N. and Husson, D.: Climatic fluctuations and sea surface water circulation patterns at the end of the Cretaceous era: calcareous nannofossil evidence, Palaeogeogr. Palaeoclimatol. Palaeoecol., 441, 152–164, doi: 10.1016/j.palaeo.2015.07.049, 2015.

Thierstein, H.R.: Late Cretaceous nannoplankton and the change at the Cretaceous–Tertiary boundary, in: The Deep Sea Drilling Project: a Decade of Progress, edited by: Warme, J.E., Douglas, R.G. and Winterer, E.L., SEPM Special Publication, 32, 355–394, 1981.

Wagreich, M., Lein, R. and Sames, B.: Eustasy, its controlling factors, and the limno-eustatic hypothesis – concepts inspired by Eduard Suess. Austrian Journal of Earth Sciences, 107, 115–131, 2014.

Watkins, D.K.: Upper Cretaceous nannofossils from Leg 120, Kerguelen Plateau, Southern Ocean, Proc. Ocean Drill. Program Sci. Results, 120, 343–370, 1992.

Wendler, J.E. and Wendler, I.: What drove sea-level fluctuations during the mid-Cretaceous greenhouse climate ? Palaeogeogr. Palaeoclimatol. Palaeoecol., 441, 412–419, 2016.

Wendler, J.E., Wendler, I., Vogt, C. and Kuss, J.: Link between cyclic eustatic sea-level change and continental weathering: Evidence for aquifer-eustasy in the Cretaceous. Palaeogeogr. Palaeoclimatol. Palaeoecol., 441, 430–447, 2016.

Williams, J.R. and Bralower, T.J.: Nannofossil assemblages, fine-fraction stable isotopes, and the paleoceanography of the Valanginian–Barremian (Early Cretaceous) North Sea Basin, Paleoceanography, 10, 815–839, 1995.

Wind, F.H.: Maestrichtian–Campanian nannofloral provinces of the southern Atlantic and Indian Oceans, in: Deep Drilling Results in the Atlantic Ocean: Continental Margins and Paleoenvironment, edited by: Talwani, M., Hay,W.W. and Ryan, W.B.F., AGU, Maurice Ewing. Ser., 3, 123–137, 1979.

Zakharov, Y.D., Popov, A.M., Shigeta, Y., Smyshlyaeva, O.P., Sokolova, E.P., Nagendra, R., Velivetskaya, T.A. and Afanasyeva, T.B.: New Maastrichtian oxygen and carbon isotope record: Additional evidence for warm low latitudes, Geosci. J., 10, 347–367, 2006.

Figure captions

Figure 1. A. Palaeogeographic reconstruction for the Maastrichtian (66 Ma) showing location of the Boreal Chalk Sea (square) and key localities discussed in the text (after Markwick and Valdes, 2004, modified). B. Palaeogeographic reconstruction of the Boreal Chalk Sea for the Maastrichtian with location of Stevns-1 (after Surlyk et al., 2003, modified).

Figure 2. Age-model for the Stevns-1 core based on the correlation of carbon-isotope curves of Stevns-1 with the astronomically calibrated ODP Site 762C and DSDP Site 525A.

Figure 3. Calcareous nannofossil climatic data and bulk stable isotopes of Stevns-1. Background colours delineate cool and warm climatic trends in the Chalk Sea. (1) Thibault et al. (2012b). (2) Surlyk et al. (2013) for details of the dinoflagellate biozonation and lithostratigraphy. (3) Rasmussen and Surlyk (2012) for the full sedimentological description of the Stevns-1 core. (4) Age model after Thibault et al. (2012a) and correlation of Fig. 2.

Figure 4. SEM picture of the Stevns-1 chalk. Sample 6146 (late Maastrichtian cooling episode, nannofossil subzone UC20b-c^{BP}, depth: 73.91m). Two of the main cool-water nannofossil taxa are shown. Bar is 10 μm.

Figure 5. Stable oxygen isotope and calcareous nannofossil data of Stevns-1 compared to data on foraminifers of South Atlantic DSDP Site 525A. The age scale is based on the correlation of carbon isotope curves between Stevns-1, DSDP Site 525A and the astronomically calibrated ODP Site 762C. La2010d: astronomical solution from Laskar et al. (2011). Benthic and planktonic foraminiferal stable isotope data from Li and Keller (1998a, 1998b) and Friedrich et al. (2009).

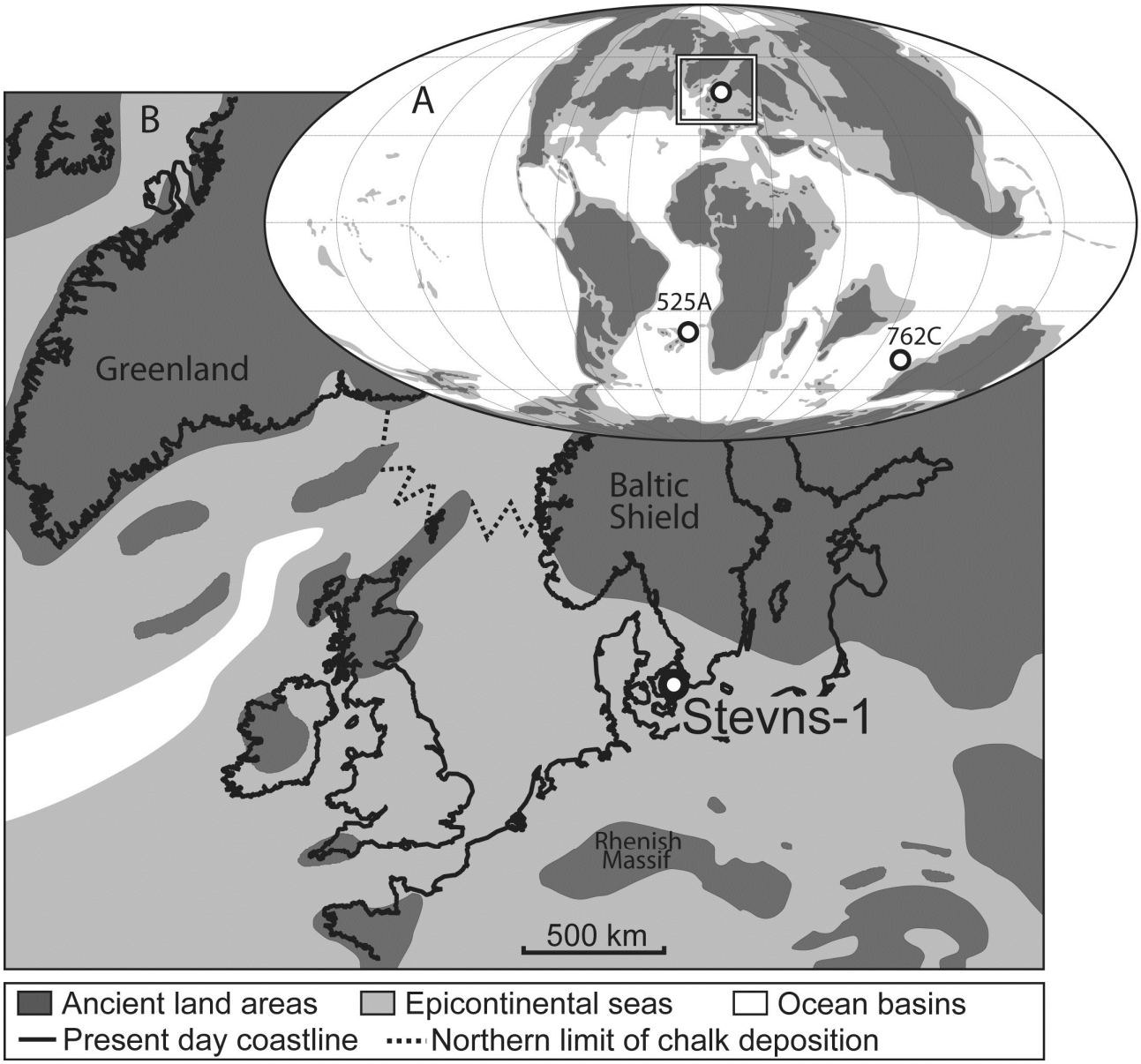

Figure 1. A. Palaeogeographic reconstruction for the Maastrichtian (66 Ma) showing location of the Boreal Chalk Sea (square) and key localities discussed in the text (after Markwick and Valdes, 2004, modified). B. Palaeogeographic reconstruction of the Boreal Chalk Sea for the Maastrichtian with location of Stevns-1 (after Surlyk et al., 2003, modified).

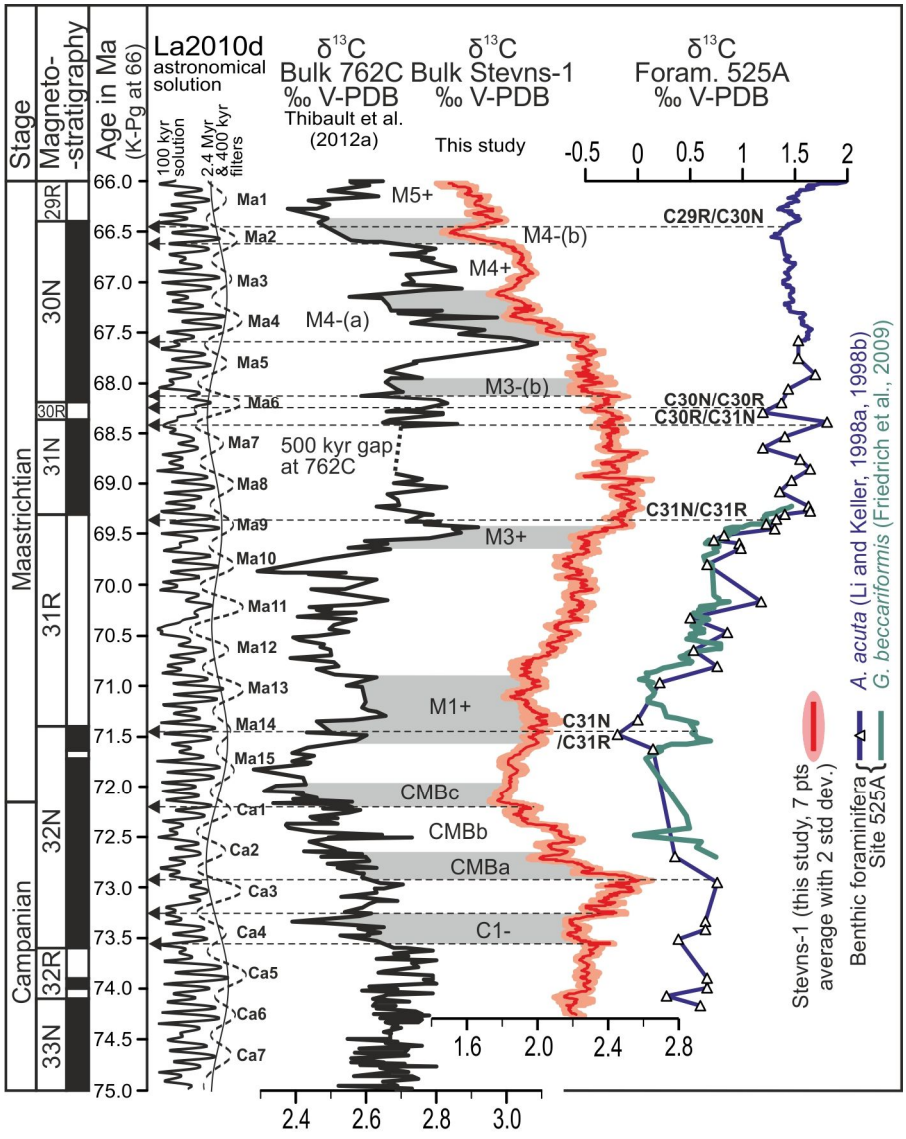

Figure 2. Age-model for the Stevns-1 core based on the correlation of carbon-isotope curves of Stevns-1 with the astronomically calibrated ODP Site 762C and DSDP Site 525A.

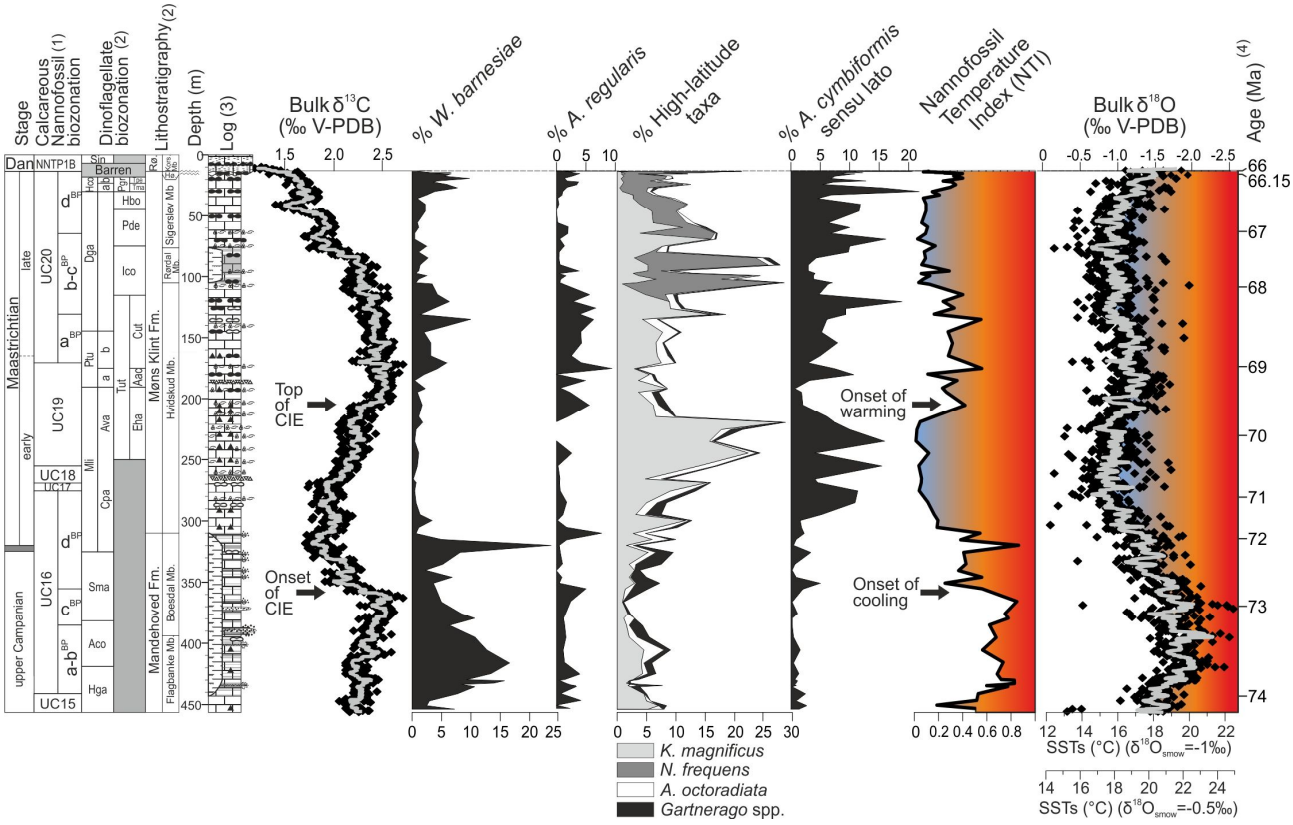

1

2 Figure 3. Calcareous nannofossil climatic data and bulk stable isotopes of Stevns-1. Background
3 colours delineate cool and warm climatic trends in the Chalk Sea. (1) Thibault et al. (2012b). (2)
4 Surlyk et al. (2013) for details of the dinoflagellate biozonation and lithostratigraphy. (3)
5 Rasmussen and Surlyk (2012) for the full sedimentological description of the Stevns-1 core. (4)
6 Age model after Thibault et al. (2012a) and correlation of Fig. 2.

7

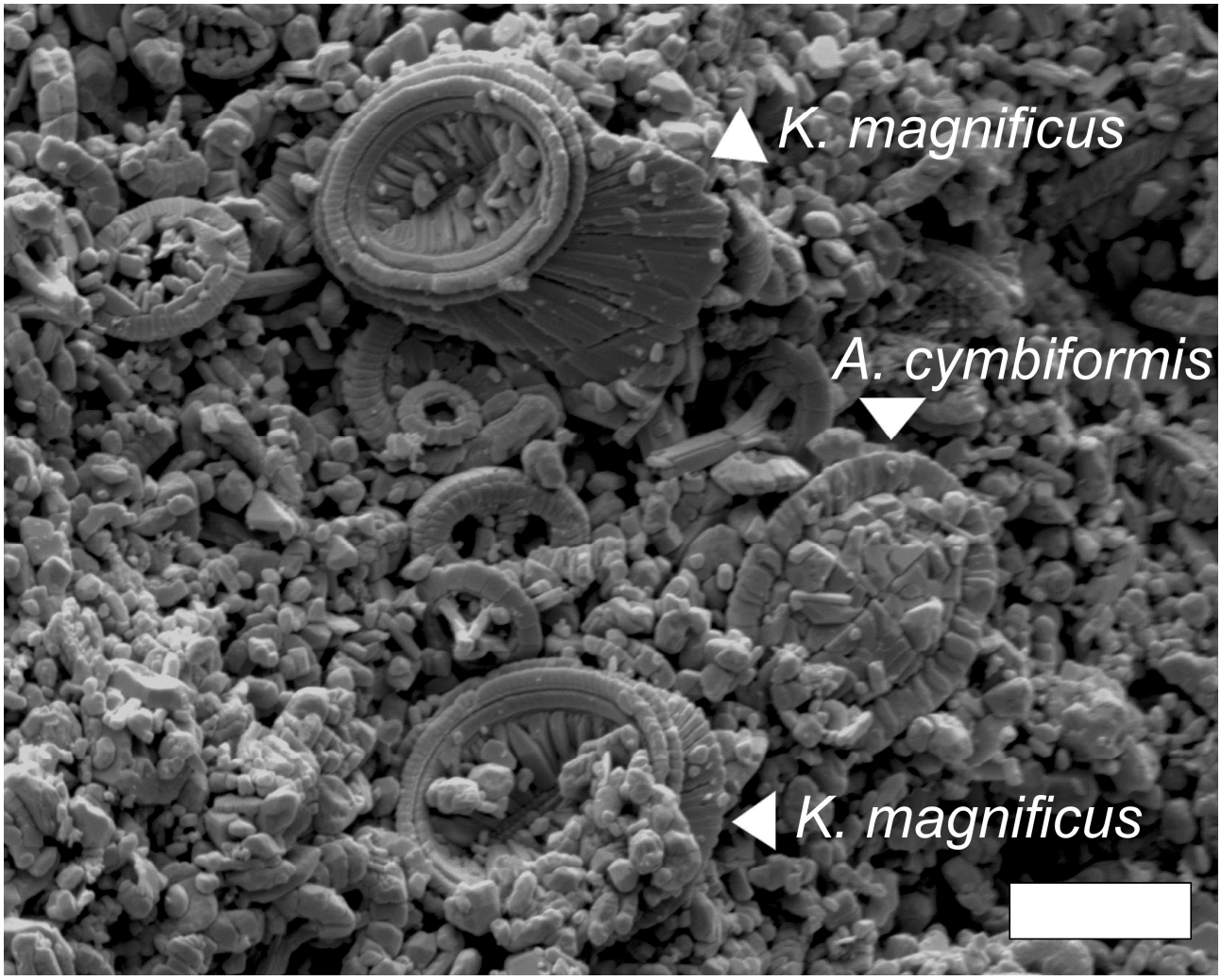

Figure 4. SEM picture of the Stevns-1 chalk. Sample 6146 (late Maastrichtian cooling episode, nannofossil subzone UC20b-c^{BP}, depth: 73.91m). Two of the main cool-water nannofossil taxa are shown. Bar is 10 μm.

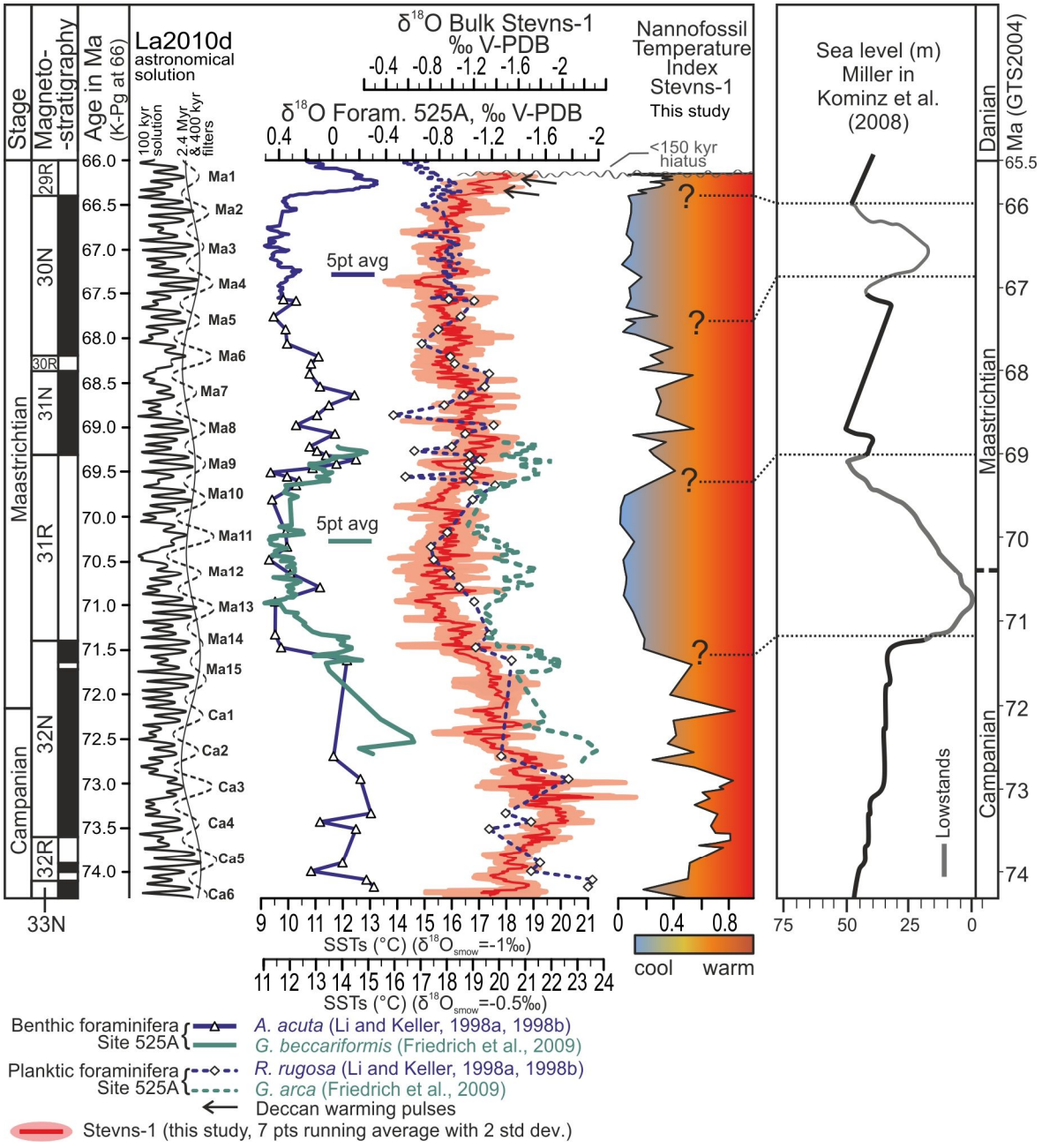

Figure 5. Stable oxygen isotope and calcareous nannofossil data of Stevns-1 compared to data on foraminifers of South Atlantic DSDP Site 525A. The age scale is based on the correlation of carbon isotope curves between Stevns-1, DSDP Site 525A and the astronomically calibrated ODP Site 762C. La2010d: astronomical solution from Laskar et al. (2011). Benthic and planktonic foraminiferal stable isotope data from Li and Keller (1998a, 1998b) and Friedrich et al. (2009).